An integrated methodology for 2x25 kV, 50 Hz traction system calculation

Evaluation of the regenerative braking effects in a HS/HC railway line

Prof. Ing. Alfonso Capasso
Dott. Ingg. Marco Ciucciarelli
Stefano Lauria

La Sapienza - University of Rome
Dipartment of Electrical Engineering

Summary

The paper describes an integrated calculation methodology which, by simulating railway traffic, allows analysis of the performance of 2x25 kV 50 Hz electric traction systems. This methodology performs a multiconductor electrical analysis of the traction circuit utilising ATP-EMTP software (Alternative Transient Program-Electromagnetic Transient Program) and therefore additionally allows calculation of electromagnetic transients and all possible failure regimes. The analyses presented refer to the application of the methodology in question to the study of a high speed railway line section in steady-state operation, with particular emphasis on the electrical and energetic effects of train regenerative braking.

1. Introduction

It is well known that the 2×25 kV, 50 Hz railway supply system in use in Italy for new High Speed/High Capacity lines ensures an outstanding performance in terms of operation capacity, reliability and flexibility as well as a substantial reduction in induced type electromagnetic interference compared to other A.C. railway supply systems in use. Fig. 1 shows the typical configuration of the 2x25 kV-50 Hz railway supply system; its peculiar structure and principle are often described in national technical literature, and therefore the present paper cites the most relevant descriptions for reference [1] [2][3].

The circuit complexity of the 2×25 kV electric traction systems, requires use of computer tools capable of solving very complex mathematical models in order to evaluate the significant electrical parameters during the design and verification phase. Since specialised software solutions for power supply system analysis were not fully suited to the analysis of electrified railway systems, custom designed software has been developed. The quantity of calculations required, due to the need to simulate various possible traffic scenarios, in some cases suggested drastically simplifying the electric system by a symmetrisation [4] and/or by reducing the number of conductors [5-7][11].

The multiconductor model proposed in [8] and [9] includes the rail distributed shunt conductance and only neglects the capacitive couplings and the autotransformer no-load currents thus giving quite precise results despite the method complexity increases with the number of trains within the line section.

Under specific operating conditions, the complete multiconductor model adopted in [10] for analysis of the interaction with the electric supply system (dissymmetry, faults), also appears to be suitably applicable to the study of electrical regimes attained in the traction circuit as a consequence of traction power demand in the simulated traffic conditions. Currently, in fact, the continuous increase in computational power potentiality has drastically reduced the requirement for simplified solutions since it is possible to calculate the steady-state condition of networks with thousand of nodes in the order of just a few seconds. Nowadays, some specialised software solutions for the analysis of electric traction systems available on the market, often lack flexibility and therefore cannot be adapted to the various design requirements; in addition, the "closed" characteristics of this type of commercial software package makes verifying the simulation methodologies and results a difficult task.

An objective was therefore set to develop a software solution capable of reliably and accurately calculating 2×25 kV, 50 Hz electric traction systems, easily highlighting electrical values of possible interest, which could also be interfaced with the typical output of railway traffic simulators in order to analyse even complex electromechanical scenarios.

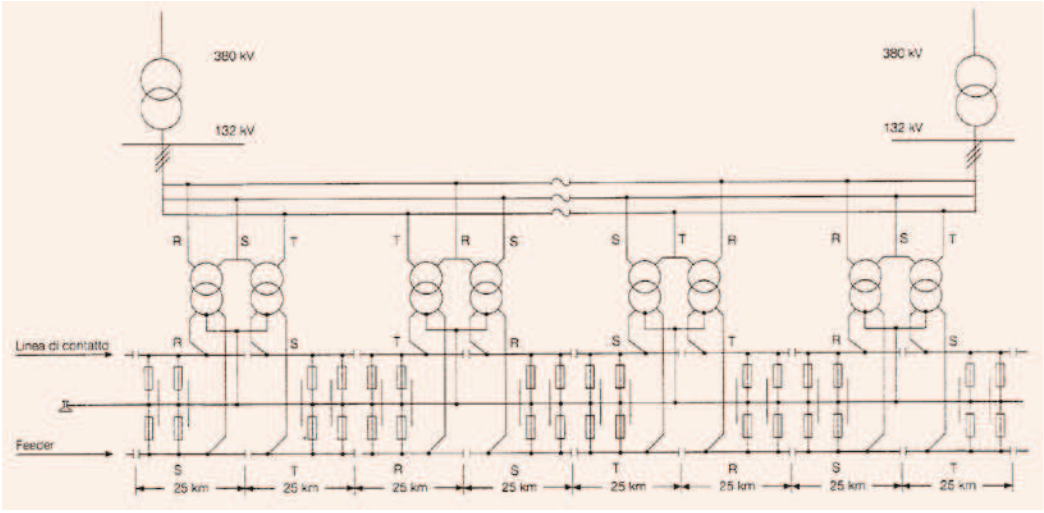

Fig.1 - General configuration of the 2x25 kV-50 Hz system (from [1])

2. The EMTP-IERSS package

The ATP-EMTP program, well known internationally as well as universally accessible, was chosen for simulation and electrical calculation of the 2×25, 50 Hz system; a new customised software was developed around this software called EMTP-IERSS (EMTP Interface for Electric Railway Systems Simulation). It should be noted that ATP-EMTP, nowadays recognised at an international level as being amongst the most reliable electric power system simulation software programs, has already been utilised at a design stage, for analysis of some types of specific electrical phenomena (faults, overvoltages) on high speed railway lines. However, the direct application of the above mentioned software program to railway lines is a complex task, with regards to the development of equivalent circuit models and, above all, with regards to pulling and processing of results; consequently its utilisation for parametric analysis purposes and / or simulation of several traffic scenarios, becomes practically impossible.

A software architecture which uses ATP-EMTP as a central solver, has been therefore developed to manage automation phases, control, result post-processing and presentation (fig. 2).

The complex structure obtained, named EMTP-IERSS (EMTP Interface for Electric Railway Systems Simulation) totally manages electromechanical simulation, processing and presentation of results interfacing within a Microsoft Windows environment with three pre-existing software programs:

- a railway traffic simulator;
- ATP-EMTP;
- Matlab.

The traffic simulator, developed in an Excel environment using macros, calculates the power drawn on the pantograph by each single train in a specified traffic scenario and within a certain time interval, step by step; the program also takes into account the line traffic (train headway along the up and down-line, starting time delay between up-line and down-line train fleets - referred to as time-shift from here on).

ATP-EMTP is utilised as the electrical network's solver routine, with additional load-flow functionality supplied by the EMTP-IERSS; finally, specific Matlab applications are used for the automatic plotting of graphs relating to the most significant electrical values.

The EMTP-IERSS structure was developed in a Microsoft Excel environment and essentially consists of several macros, in other words executive codes written in VBA (Visual BASIC for Application).

This allows development, in a single file, of a structure based on the creation of several databases where data and results obtained from the macros can be saved for checking, post-processing and possibly archiving.

The VBA environment allowed quick development of client interfaces for improvement of the entire software but most notably it showed a very high database and file access speed. The calculation phases can be summarised as:

i - interfacing with the traffic simulator;

ii - ATP-EMTP based load flow calculations;

iii - pulling of results.

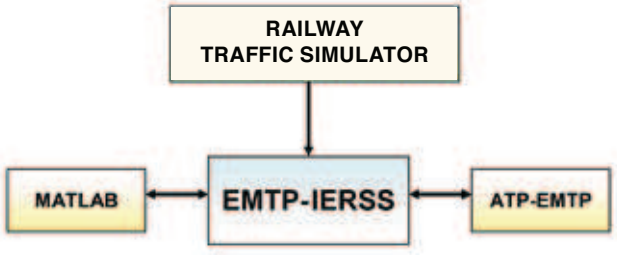

Fig. 2 - Block diagram of the EMTP-IERSS package

3. ATP-EMTP modelling of the electric supply system

The equivalent electric circuit of a two-track 2x25 kV-50 Hz high-speed/high-capacity railway line is composed of 14 conductors in a given section (fig. 3), namely rails (R1P,R1D, R2P, R2D), overhead ground wires (CTP, CTD), buried linear grounding conductors (DIP, DID), feeders (FDP, FDD), messenger wires and contact wires (COP, COD). Grounded conductors are also bonded at regular intervals by means of equipotential connections.

The adoption of a lumped-parameters "Pi" model is widely justified, for steady-state power frequency analyses, by the short length of the single line element with respect to the different 50 Hz wavelengths of the railway line, ranging from 6000 km for the overhead conductors to 94 km for the rails.

As far as conductor arrangement is concerned the following 4 typological sections have been taken into consideration:

- embankment/cutting;
- viaduct;
- natural tunnel;
- artificial tunnel.

Messenger wires and contact wires were replaced by a single equivalent conductor, suitably located, thus reducing the equivalent circuit complexity to 12 conductors; sags of messenger wires, overhead ground wires and feeders were calculated for a temperature of 55 °C. Particularly important is the model implemented for rails and buried linear

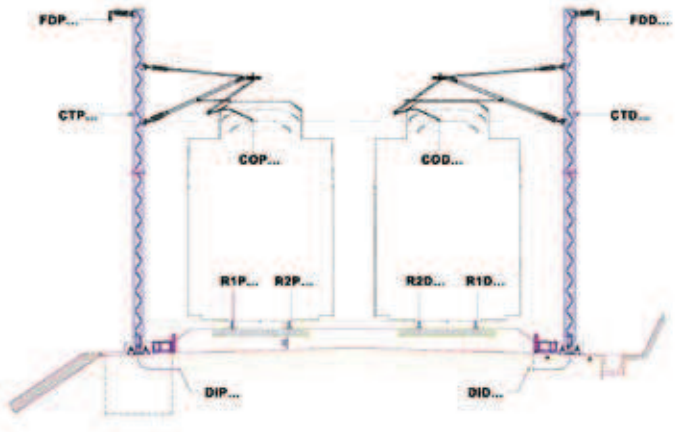

Fig. 3 - Embankment cross-section of the 2x25 kV-50 Hz line

Multiconductor line model consists of cascaded lumped-parameter Pi-circuits (fig. 4), each one representing a 250 m line section (equipotential bonding connections occur at multiples of 250 m, i.e. 750 and 1500 m) that is solved with a specific EMTP code.

grounding conductors. Each single rail is represented by an equivalent non-ferromagnetic cylindrical conductor of 220 mm diameter (i.e. the perimeter of a UNI 60 rail), of which the internal impedance accounts satisfactorily for

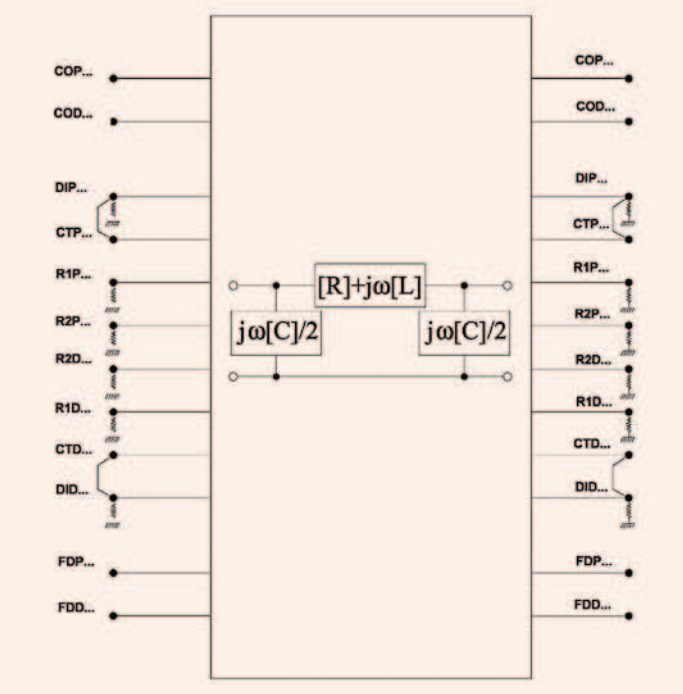

Fig. 4 - Synthetic representation of a "nominal Pi" circuit and the "equivalent multipole"

the 50 Hz skin effect of the rail. Shunt conductance, being the running rails included in a transmission line model with conductors usually insulated from ground, was simulated by linear lumped resistances connected to ground at the ends of each 250 m Pi-circuit. The adopted representation is widely accepted in most real cases that can be found in the electric traction circuits [12], with the exception of some specific situations where rails are poorly insulated from ground (i.e. g=10 S/km) or in case of high resistivity soil (ρ=4000 Ωm).

The equipotential connections between overhead ground wires and buried linear grounding conductors (they are connected to the contact line masts every 50-60 meters) are simulated at 250 m intervals; overhead ground wires running along the up and down lines are bonded every 750 m (three cascaded Pi-circuits). The following elements have been moreover included in the equivalent circuit:

i - inductive connections every 1500 m;

ii - transformers and autotransformers, represented by standard models according to the relevant rating values;

iii - train itself, represented as a lumped impedance connected between contact wire and rails at one end of a Pi-circuit; the complex impedance evaluated by EMTP-IERSS can have any argument, allowing to reproduce a four-quadrant operation in the (P,Q) plane; as the impedance can only be connected at the Pi-circuit ends, the simulated position of the train along the line is affected by a ±125 m approximation.

4. Load-flow implementation

Although the input for the train "electric" modelling is represented by the active power value as given by traffic simulator, the load-flow algorithm takes into account the real P-V limit curve that defines the relation between active power demand and pantograph voltage. figs.5 and 6 show respectively the two cases of traction and recovery braking for an ETR500 train. As far as braking is concerned, the standard curve implemented in most simulations is named "Case 1" in fig. 6 while "Case 2" and "Case 3" variations refer to some of the simulations detailed in §6.

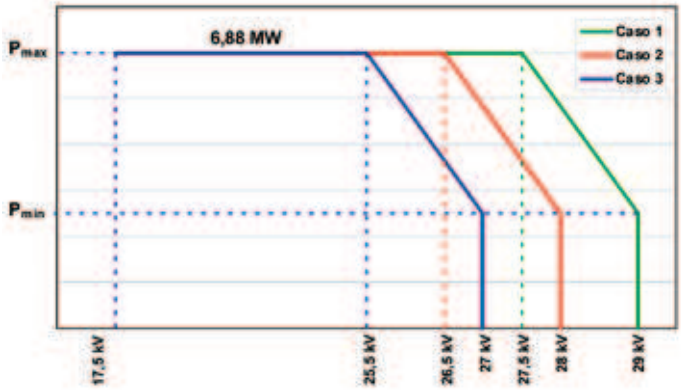

Fig. 5 - Active power demand - pantograph voltage limit curve of the ETR500AV train (traction)

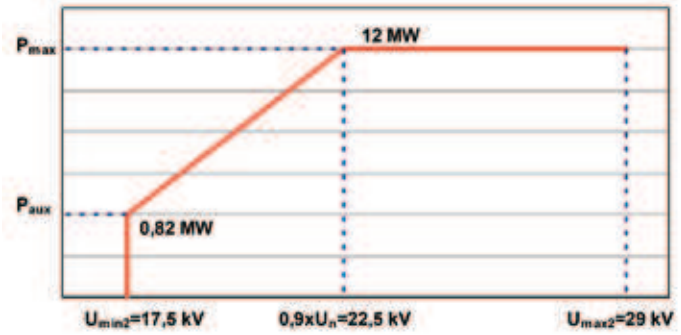

Fig. 6 - Active power demand-pantograph voltage limit curve of the ETR500AV train (braking phase) ("Case 1": standard characteristics, "Case 2" and "Case 3" modified characteristics, see §6)

Train electric modelling by means of active and reactive power demands (constant or variable in a defined range of the pantograph voltage) makes the equivalent impedance non-linear thus requiring the utilisation of specific iterative load flow algorithms for the solution of the electric network non-linear equations. Radial operation of the 2x25 kV-50 Hz system suggested the utilisation of a specific load flow algorithm for the electric network solution (a linear network with the exception of the loads, that is the trains); network solution is achieved by iteratively adjusting the train equivalent impedances, according to the voltage values calculated in the preceding calculation step, till reaching the convergence; (a modification of the previous algorithm, often named "Y^{BUS}" and commonly used in the distribution network, considers the variation of the nodal current injections equivalent to the loads). The relevant algorithm is illustrated in fig. 7. That iterative procedure accepts maximum tolerances of 0.5% with respect to the active power constraints set by the traffic simulator.

The adopted algorithm is very robust, achieving always convergence up to the physical loadability limit of the line; in addition it can be easily implemented

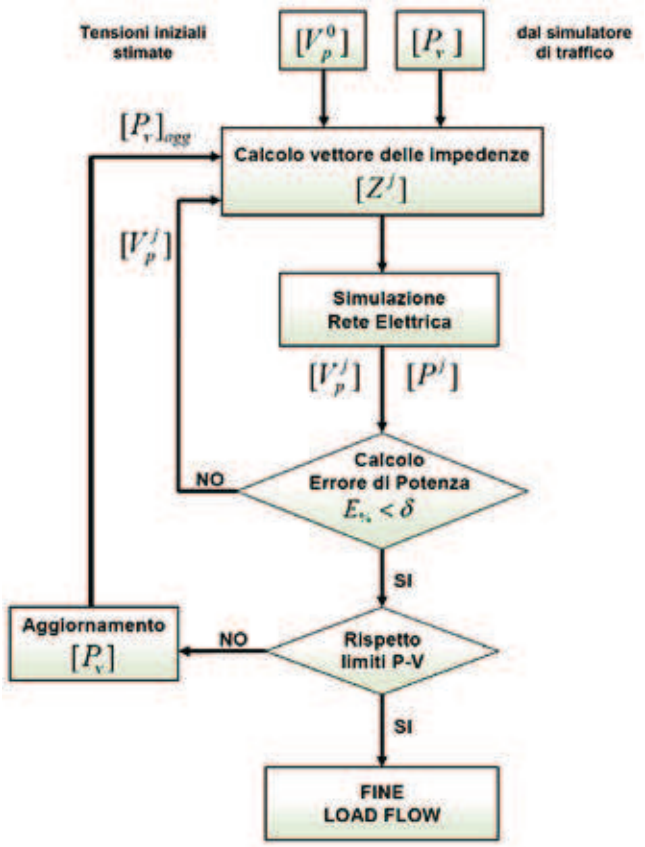

Fig. 7 - Flow-chart of the implemented load flow algorithm

by using the ATP-EMTP initialization (phasor) routine as network solver. As shown by flow-chart in fig. 7, the proposed software calculates the initial value of the impedance vector while the ATP-EMTP core software solves iteratively a multiconductor and unsymmetrical linear network, the constant impedance loads being recalculated in each single step of the iterative procedure. Load-flow algorithm is endowed with an outer control loop (fig. 7) taking into account the real traction characteristics of figs. 5 and 6; this loop modifies the active power constraint of a given train when the pantograph voltage is such to impose a voltage-dependant behaviour of power demand instead of a constant power behaviour.

An early experimental verification of the EMTP-IERSS software was carried out by comparing the simulation results with some power, energy and voltage measurements in the Chivasso ESS. Despite the low sampling frequency of the available fixed instrumentation it was possible to verify the good match, in terms of energy demand, with the calculation results.

5. Application to the study of the Torino-Novara HS/HC railway line

The EMTP-IERSS calculation procedure was applied to the operation simulation of the high-speed/high-capacity railway line sub-section Torino-Novara, part of the overall project of the Torino-Milano HS connection, about 125 km in length. The Torino-Novara sub-section, covering a distance of about 91 km almost completely outdoor, was put in operation on February 2006. The analysis here proposed refers to the 2x25 kV-electrified line section between the Torino POC (AC/DC separation Point) at km 2.250 and the starting point, at km 84.000, of both the Novara Node interconnection and the connecting section with the 3 kV d.c. system, of which the relevant POC (AC/DC separation Point) is located at km 85.300.

Fig. 8 shows the single-line diagram of the 25 kV-50 Hz power supply system under normal operating condition, including the specific location of ESSs and PAPs (Paralleling and Auto-Transformation Posts) along the Torino-Novara high-speed/high-capacity railway line.

Under normal operation conditions only one 60 MVA transformer per ESS supplies both the traction circuits north and south of the ESS itself. In all PAPs only one autotransformer is in operation with the exception of the Alice Castello PAP where a phase change occurs, requiring the operation of both autotransformers being one connected to the north traction circuit and the other to the south circuit.

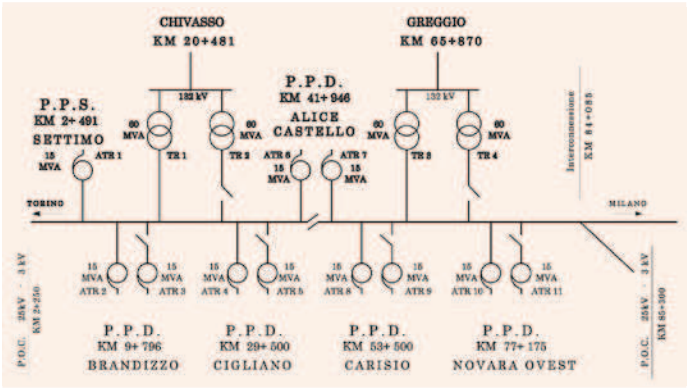

Fig. 8 - Single-line power supply diagram of the 2x25 kV – 50 Hz HS/HC Torino-Novara railway line

Analysis results here presented refer to one of many simulated traffic scenarios, namely the scenario with 15 minutes train headway and 0 minutes time-shift between trains entering the line at the two opposite ends. As shown by the train path of fig. 9, this turns to have at most two trains on each track at any given instant.

Figure 10 shows, versus time, the overall active power and energy demand for the traffic scenario under consideration, whereas figs. 11 and 12 respectively show the active power demand and the pantograph voltage of a given train (TAD in fig. 9) running the up-line from Settimo T. to the Novara Ovest interconnection.

It is moreover obviously possible to achieve other quantities such as power and current values in the different PAPs; in general the program can access and evaluate all the electrical quantities of the supply system. As an exemplification of the achievable output variety, fig. 13 shows the active power demand and losses of TR3 transformer in the Greggio ESS, whereas fig. 14 shows the track voltage at the TAD train location, measured with respect to the voltage of the system reference node, that is the remote ground.

6. Analysis of regenerative braking effects

The regenerative braking advantages are well known in the subway traction field, due to extensive studies and a long dated-back operation experience (see for instance [13]). The frequent starting/stopping cycles consequent to the presence of numerous stations, together with the line planimetric and

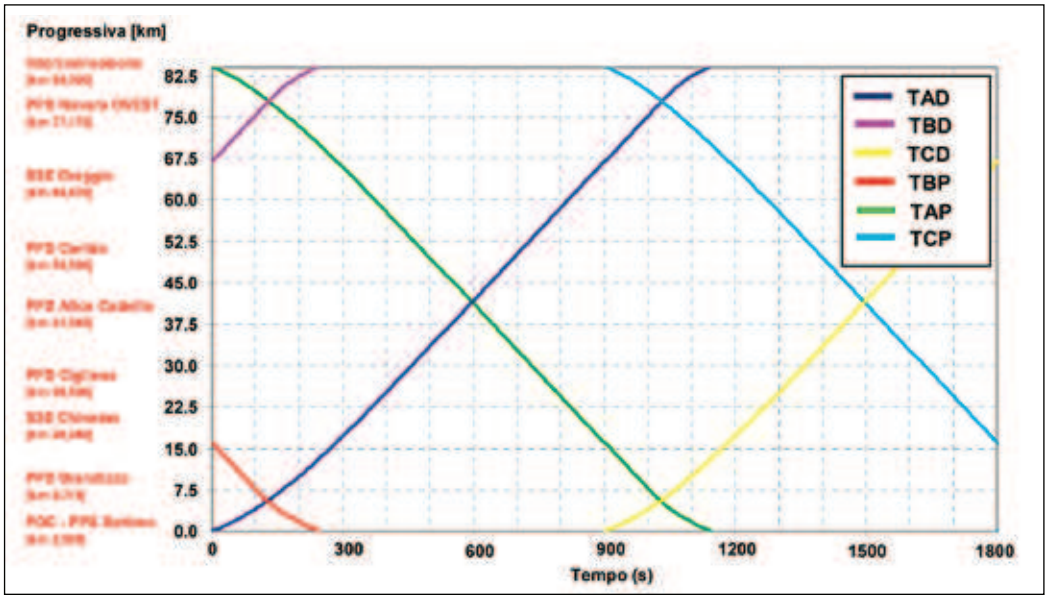

Fig. 9 - Train Path for the reference traffic scenario (15 minutes headway, 0 minutes time-shift)

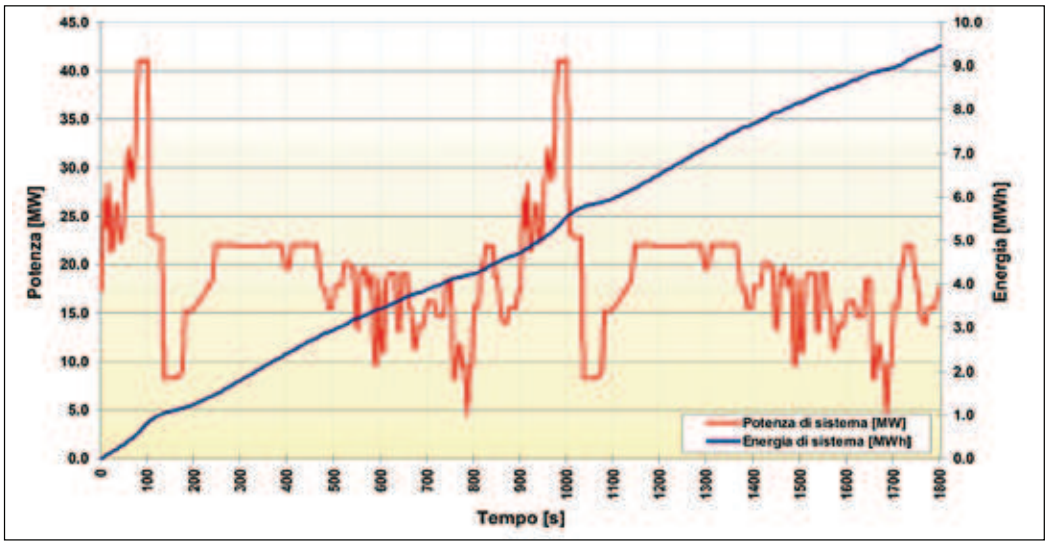

Fig.10 - Overall power ed energy demands for the reference traffic scenario (15 min. headway, 0 minutes time-shift)

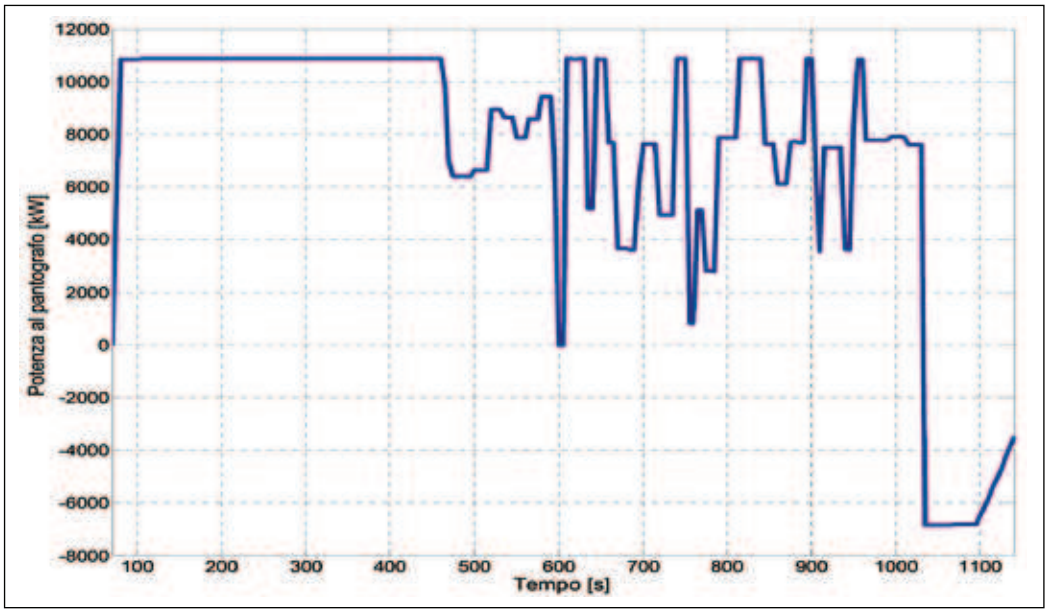

Fig. 11 - Active power demand at pantograph of train TAD of Figure 9 vs. time

altimetric characteristics, imply that during rush hours the average recovered energy can even reach 15-20% of total consumption.

In high-speed railway lines, differently from subway lines, braking phases only occur at the end of the line sections or at the line junctions/interconnections, also as a consequence of low line slopes, very large curve radii and an almost complete absence of intermediate stops. The energy balance of regenerative braking in high-speed railways has been then largely overlooked, attention being mostly focused on savings deriving from running optimization [14].

6.1 Effects of line traffic

The EMTP-IERSS software package allows to evaluate all traffic-related issues when studying regenerative braking in a.c. traction systems, taking into account all the electromechanical aspects characterizing this phenomenon.

The reference case in fig. 9 (15-minutes headway and 0-minutes time-shift) makes it possible to verify that the positions of two different trains within the line and the possible simultaneous occurrence of braking and acceleration phases have a significant influence on this phenomenon.

The consideration of both the traction supply system diagram of the Torino-Novara line section (fig. 8) and the Train Path of fig. 9, reveals that only two trains, TAD and TBP, fall inside the line section from Settimo T. POC (AC/DC separation Point) to Chivasso ESS, between t=70 s and t=180 s; in particular train TAD running the down line is in traction phase while train TBP running the up-line is in braking phase. Paralleling connections between tracks allow the exchange of the excess braking energy

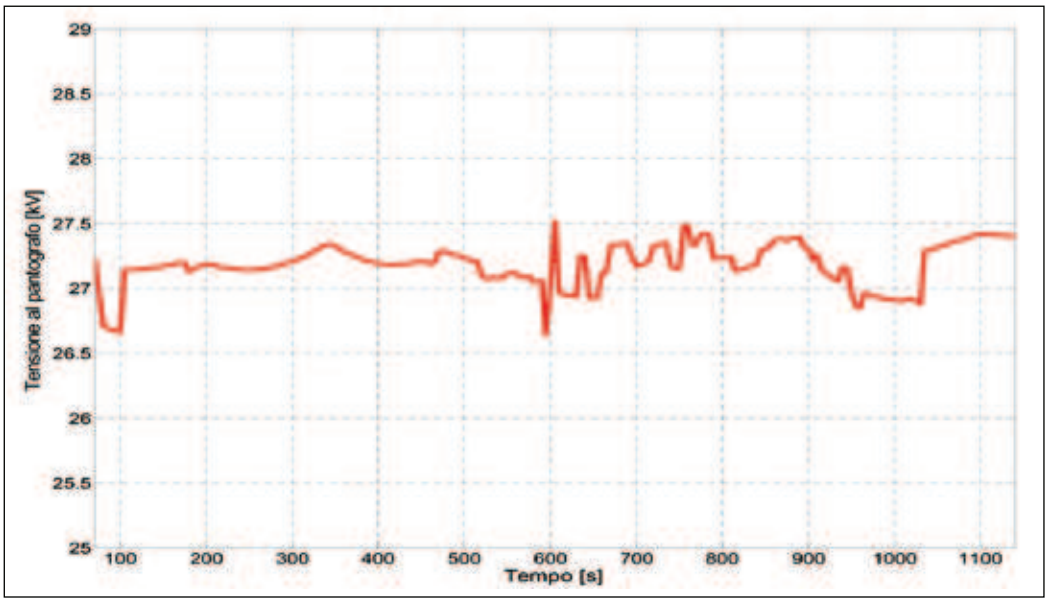

Fig. 12 - Pantograph voltage for train TAD of Figure 9 vs. time

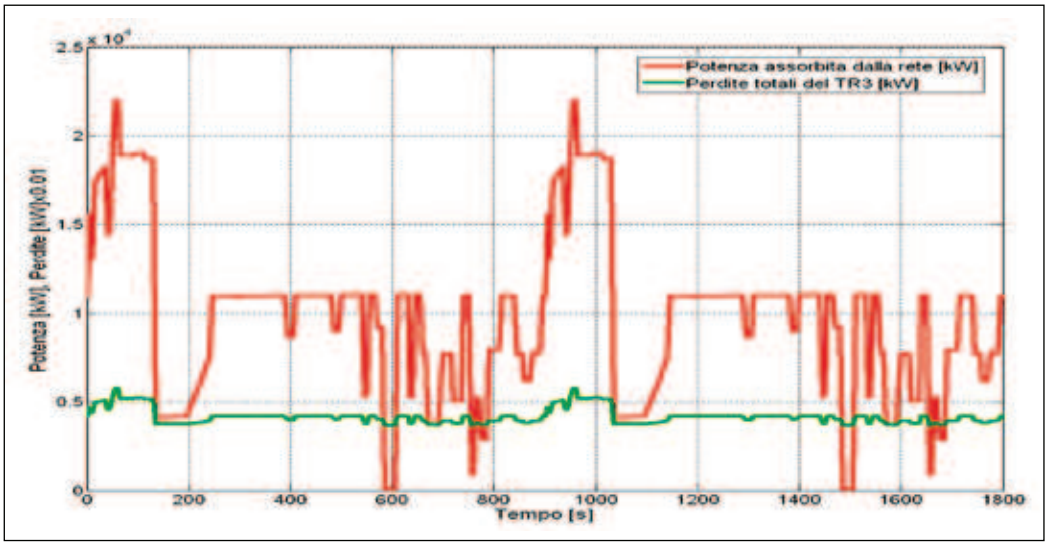

Fig. 13 - Active power demand and losses of transformer TR3, Greggio ESS

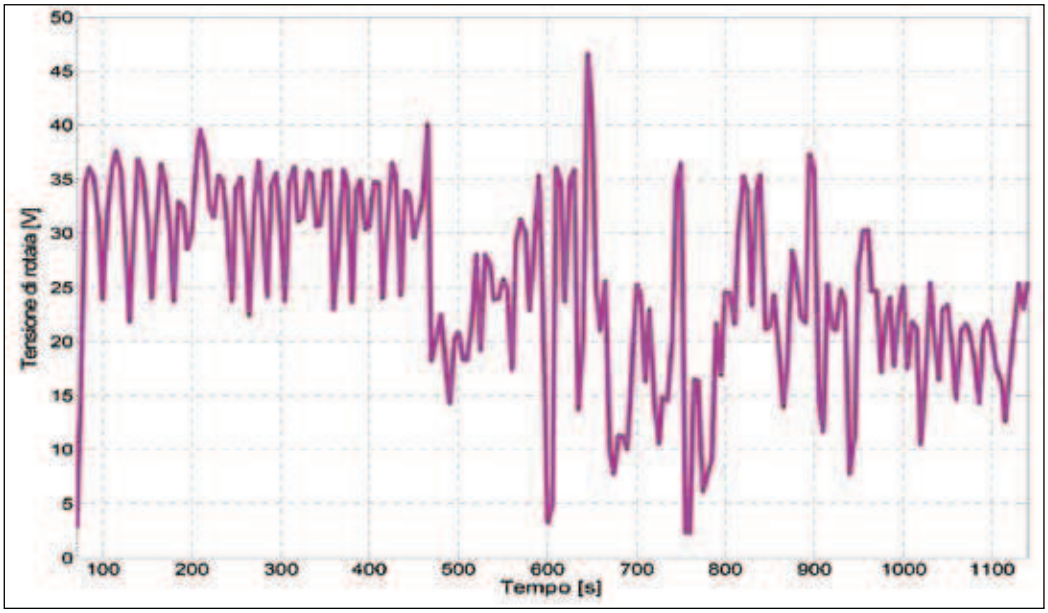

Fig. 14 - Track voltage at the TAD train location, vs. time

between the Up and Down lines and make the line fully receptive in terms of braking energy recovery capability. Fig. 15 shows both power demand and pantograph voltage increase of the TAD train, that is in regenerative braking phase between t=1030 s and t=1140 s, anyway respecting the limit curve of fig. 6.

A parametric analysis was subsequently performed on the HS/HC Torino-Novara line section by varying both train headway and time-shift between up-line and down-line train fleet, in order to evaluate the influence of main traffic parameters on the recovered energy amount. The parametric analysis results are synthetically shown in fig. 16, where the regenerative braking efficiency (recovered energy/theoretically recoverable energy), a significant measure of the line receptivity, is plotted as a function of both traffic variables (headway and time-shift), being the theoretically recoverable energy equal to train kinetic energy variation as given by traffic simulator, net of conversion efficiency.

Figs 17 and 18 show the cross-sections of the surface in fig. 16 representing the braking efficiency curves versus time-shift (for a 15-minutes headway) and respectively versus headway (for a 0 minutes time-shift). When line receptivity is low due to a higher headway, pantograph voltage could reach the limit beyond which the regenerative braking energy is partially dissipated on rheostats (see fig. 6), leading to a decrease in the energetic efficiency as shown in fig. 16.

This decrease is influenced by both traffic conditions and planimetric and altimetric characteristics of the line section; in the present case, characterised by the absence of intermediate stops and by

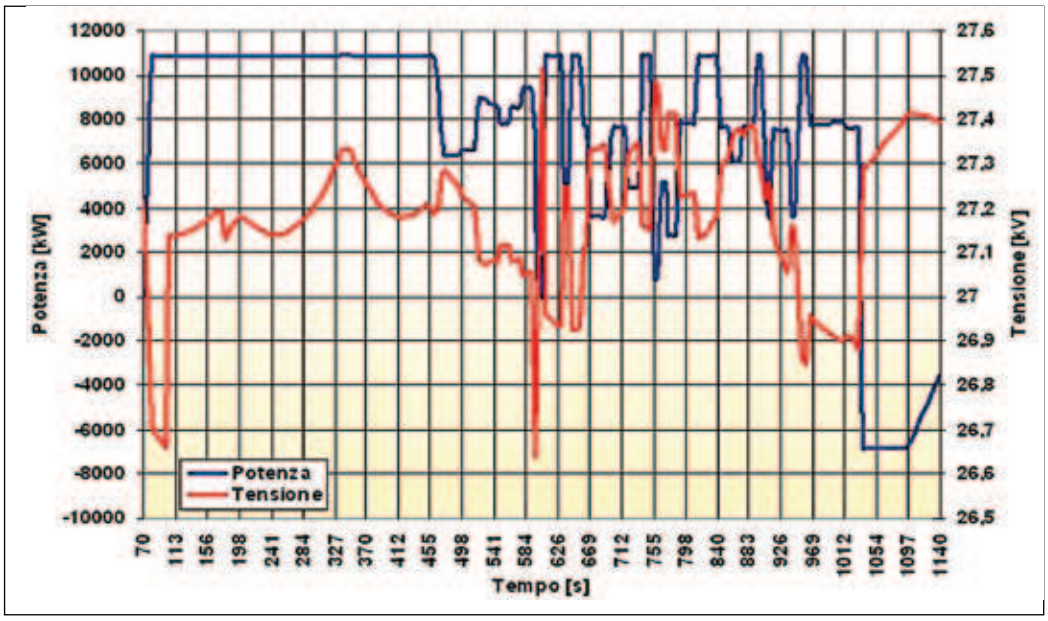

Fig. 15 - Pantograph active power demand and voltage of the TAD train (base case)

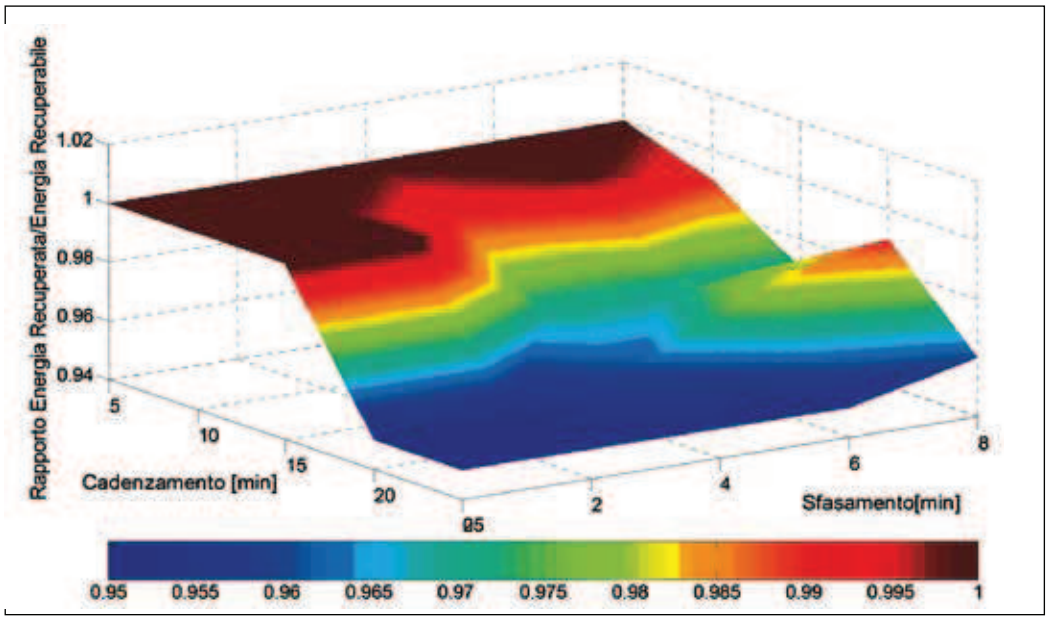

Fig. 16 - Recovered energy/recoverable energy ratio as a function of traffic parameters (headway and time-shift)

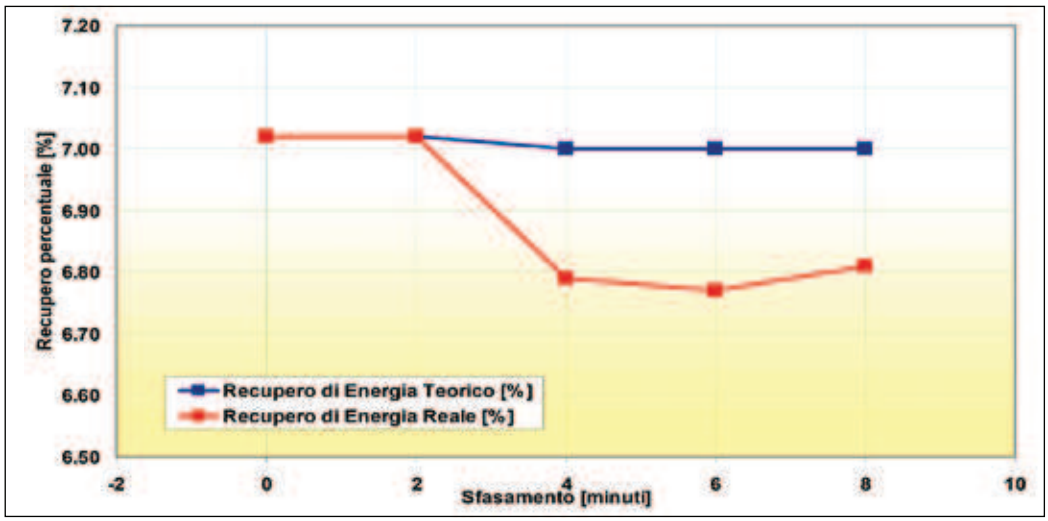

Fig. 17 - Comparison between theoretical and actual (simulated) energy recovery as a function of time-shift (15 minutes headway)

a mainly flat and straight layout, braking efficiency is always greater than 0.95. Table 1 finally reports the main results of simulations performed by varying the headway by 5-minute increments in the (5-25) minutes range, as well as by varying the time-shift by 2-minute increments in the (0-8) minutes range. Overall recovered energy is comprised between 4% and 8% of overall train demand according to the different traffic conditions.

This parametric analysis also shows that receptivity is unaffected by the time-shift as long as the headway does not exceed 15 minutes, being all the recovered energy used in the railway line (i.e. drawn by other trains) without any feedback to the HV network through the ESSs. For headways exceeding 20 minutes, receptivity falls sharply, because in this case there are no trains with opposite running phases (acceleration and braking) along the same line, being the braking energy transfer only possible between trains running the two different electrically connected lines.

As far as this energy transfer is concerned, for headways greater than 20 minutes, the time-shift of the train entrances in the up-line and down-line is even more important as it can influence the possible contemporary presence of two trains on the same sub-section in opposite running phases.

The recovered energy, when not occasionally drawn by the train running the opposite line, is fed back into the HV supply network, obviously net of line losses and rheostatic dissipation energy limiting the pantograph voltages).

6.2. Influence of line voltages

Voltage drops associated to power flows in a.c. traction lines, especially

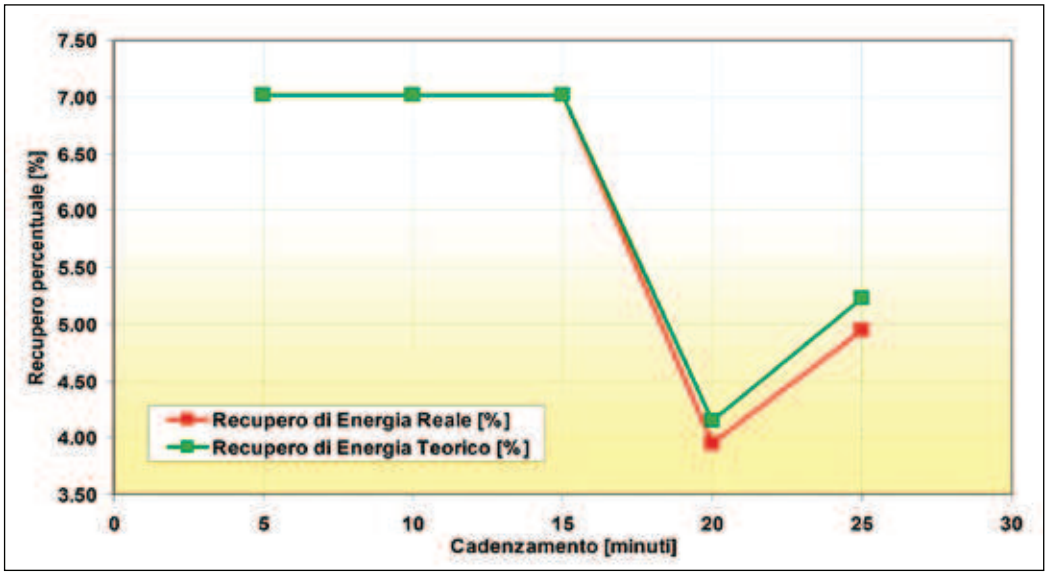

Fig. 18 - Comparison of theoretical and actual (simulated) energy recover as a function of train headway (0 minutes time-shift)

N°	Headway [min]	Phase displacement [min]	Overall Energy Demand of the ESSs [MWh]	Overall Energy demand of the trains [MWh]	Transmission efficiency η_{RE} [%]	Recovered energy [%]	Recoverable energy [%]	Recovered/recoverable energy ratio
1	5	0	28.2	28.0	99.20	7.0	7.0	1.00
2	10	0	14.2	14.0	98.87	7.0	7.0	1.00
3	15	0	9.5	9.3	98.57	7.0	7.0	1.00
4	20	0	8.0	7.9	98.39	4.0	4.2	0.95
5	25	0	6.4	6.3	98.10	5.0	5.2	0.95
6	5	2	28.2	28.0	99.19	7.0	7.0	1.00
7	10	2	14.2	14.0	98.84	7.0	7.0	1.00
8	15	2	9.5	9.3	98.55	7.0	7.0	1.00
9	20	2	7.7	7.6	98.34	4.1	4.3	0.95
10	25	2	6.0	5.9	97.99	5.3	5.5	0.95
11	5	4	28.2	28.0	99.17	7.0	7.0	1.00
12	10	4	14.2	14.0	98.84	6.9	7.0	0.99
13	15	4	9.5	9.4	98.49	6.8	7.0	0.97
14	20	4	7.4	7.2	98.28	6.2	6.5	0.96
15	25	4	5.7	5.5	97.88	5.6	5.9	0.95
16	5	6	28.2	28.0	99.19	7.0	7.0	1.00
17	10	6	14.2	14.0	98.85	7.0	7.0	1.00
18	15	6	9.5	9.4	98.51	6.8	7.0	0.97
19	20	6	7.3	7.1	98.25	6.4	6.6	0.98
20	25	6	5.5	5.4	97.85	5.8	6.1	0.95
21	5	8	28.2	28.0	99.16	7.0	7.0	1.00
22	10	8	14.2	14.0	98.85	7.0	7.0	0.99
23	15	8	9.5	9.4	98.52	6.8	7.0	0.97
24	20	8	7.1	7.0	98.26	6.6	6.7	0.99
25	25	8	5.4	5.3	97.82	7.9	8.3	0.96

Table 1 - Summary of performed simulations results

P-V simulated curve under braking condition (see figure 6)		Case 1	Case 4	Case 2	Case 3
Overall energy demand of the ESSs	[MWh]	9,47	9,82	9,76	10,11
Overall energy demand of the running trains	[MWh]	9,33	9,33	9,63	9,99
Overall recovered energy	[MWh]	0,65	0,65	0,36	0,00
Overall recoverable energy	[MWh]	0,65	0,65	0,65	0,65
Transmission efficiency	[%]	98,57	95,02	98,61	98,69
Real energy recovery	[%]	7,02	7,02	3,74	0,00
Theoretical energy recovery	[%]	7,02	7,02	6,80	6,56

Table 2 - Energy-related results of the simulations

during regenerative braking when train power factor is approximately close to unity ($\cos\varphi=1$), are significantly affected, differently from the HV transmission system case, by line resistance (not negligible with respect to line reactance) with consequent variations of the line voltage r.m.s. value.

For high no-load voltage values in the ESS and low traffic conditions, pantograph voltage of the braking train could rise up to the maximum allowable limit (29 kV) possibly causing undue trips of pantograph maximum voltage protection relays of other trains entering the same line section.

In principle, the standard train braking P-V curve ('Case 1' in fig. 6) could be modified by reducing the knee voltage U^{max1} and the limit voltage U^{max2}. The effects of such modifications on the recovery braking characteristics have been here evaluated by simulating the same 'base' traffic scenario with the two other braking characteristics of Figure 6, as achieved by reducing the U^{max1} and U^{max2} values by either 1 kV ('Case 2' in fig.6) or 2 kV ('Case 3').

Figs. 19 and 20 show, for the three considered cases, the active power demand and, respectively, the relevant pantograph voltage of train TAD, with a particular attention to the braking time-window. Cut of the allowable braking voltages, while causing only a slight reduction (less than 1%) in the pantograph voltage strongly reduces the power reinjection from the braking train and then the recovered energy. Simulation results presented in Table 2 show that the recovered energy amount drops from 100% ('Case 1') to 70% ('Case 2') till to 0 ('Case 3').

Simulation results show that the modification of the braking limit curve under light load conditions

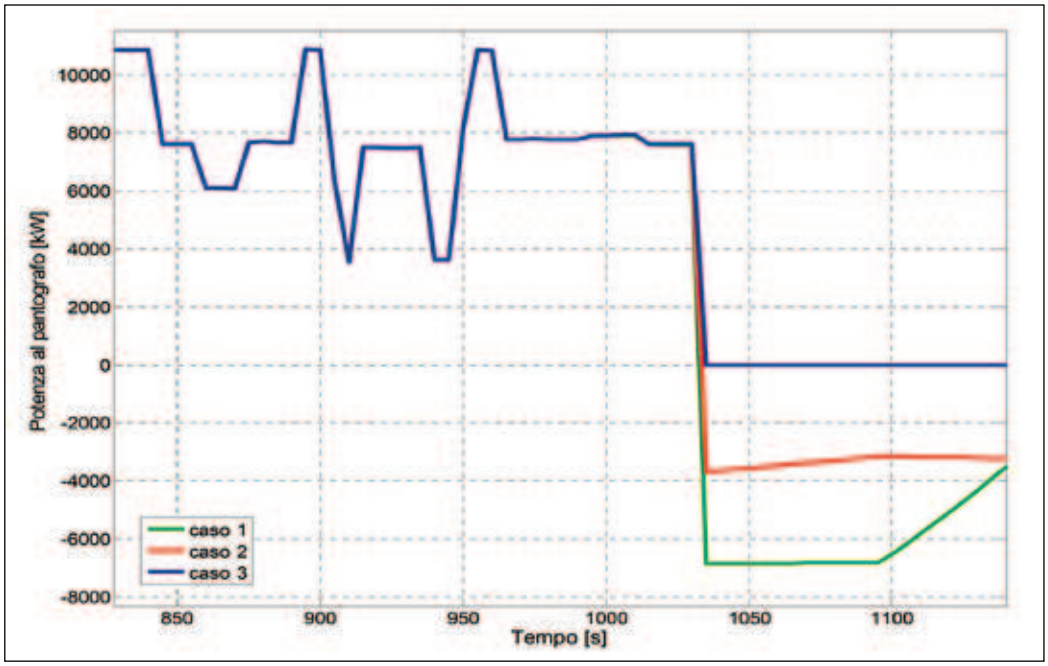

Fig. 19 - Active power demand at the pantograph of TAD train versus Time, for the three different braking curves of fig. 6

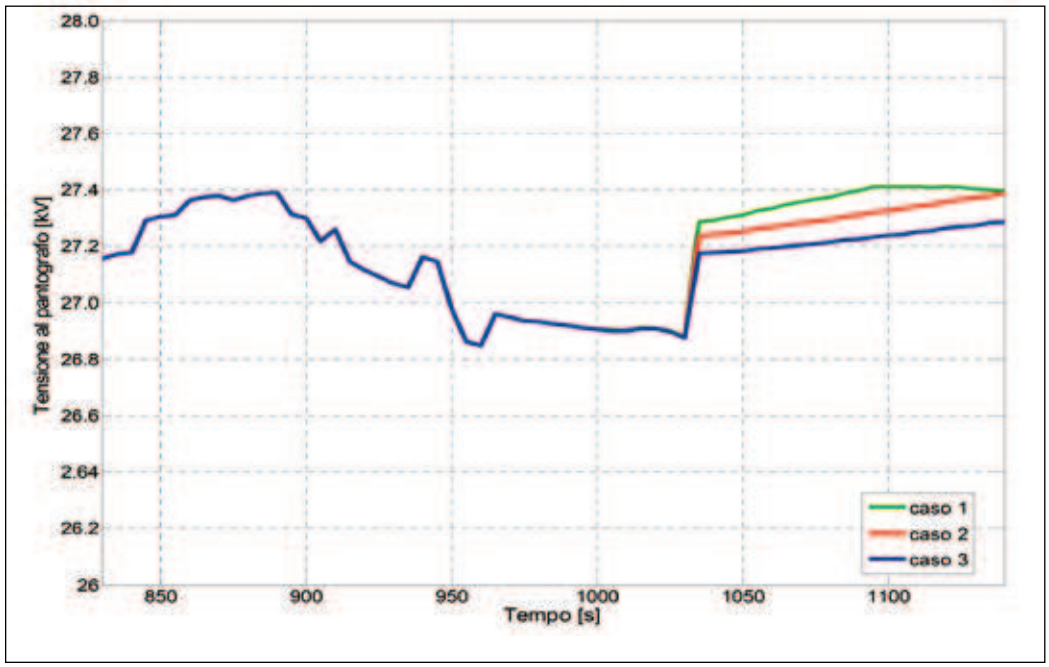

Fig. 20 - Pantograph voltage of TAD train versus Time, for the three different braking curves of fig. 6

determines a huge reduction of regenerable energy, against a small reduction of pantograph voltages. In order to reduce line voltages in light load conditions without compromising energy recover, the supply system can be operated with slightly lower no-load supply voltages in the ESSs, while keeping the "nominal" limit P-V braking curves.

The real effect of this measure was verified by simulating the 'base' electromechanical scenario and setting at 26.5 kV the ESSs no-load voltages ('Case 4' in Table 2). Case 4 of Table 2 shows that lower no-load voltages in the ESSs turn into an increase of the ESSs overall energy demand, if compared with Case 1 results, as a consequence of the reduction (around 3%) of the 25 kV transmission efficiency; on the other hand, regenerative braking achieves 100% energy recovery while line voltages are kept fully compliant with the European Interoperability Technical Specification limits [15].

N°	Headway [min]	Time Shift [min]	Overall energy demand of the ESSs [MWh]		Overall energy demand of the trains [MWh]		Transmission efficienty η_{SE} [%]		Recovered energy [%]		Recoverable energy [%]		Recovered/recoverable energy ratio	
Configuration TE			1TR/SSE	2TR/SSE	1TR/SSE	2TR/SSE	1TR/SSE	2TR/SSE	1TR/SSE	2TR/SSE	1TR/SSE	2TR/SSE	1TR/SSE	2TR/SSE
3	15	0	9.5	9.5	9.3	9.3	98.57	98.17	7.0	7.0	7.0	7.0	1.00	1.00
8	15	2	9.5	9.5	9.3	9.3	98.55	98.14	7.0	7.0	7.0	7.0	1.00	1.00
13	15	4	9.5	9.5	9.4	9.4	98.49	98.10	6.8	6.6	7.0	7.0	0.97	0.94
18	15	6	9.5	9.5	9.4	9.4	98.51	98.10	6.8	6.6	7.0	7.0	0.97	0.94
23	15	8	9.5	9.5	9.4	9.4	98.52	98.12	6.8	6.6	7.0	7.0	0.97	0.94

Table 3 - Results of simulations with 15 minutes headway and ESS "neutral sections" in open position

6.3. Influence of the traction supply system configuration (switching arrangements) on the network receptivity

Results of the above illustrated parametric analysis are obviously related to the simulated traction supply configuration as the closure of the SSE neutral sections and the utilisation of only one supply transformer, (fig. 8), make the traction circuit electrically continuous along half the line length (that is about 50 km); the energy injected by braking trains can thus be drawn by other "electrically near" trains. This network configuration makes the railway line capable or partially capable to directly use the braking energy, even for a train separation distance of about 50 km. It can then guarantee, for train headways below 20 minutes, a sufficient traction demand that makes the braking energy transmission back to the HV network not necessary.

An energetic analysis of regenerative braking effects has been considered quite interesting; in particular the above illustrated results have been compared with the results achieved with a different traction circuit configuration where the ESSs are operated with their neutral section in "open" position and both the transformers in operation.

In this specific case the traction supply line is subdivided into 4 electrically independent sections which can not directly exchange any braking energy. Table 3 shows the comparison of the energy-related simulation results for the two supply configurations, considering a 15-minutes headway and a time-shift between trains on the opposite lines (up and down) varying from 0 up to 8 minutes. The energetic parameters differences reveal to be small but anyway significant of the actual electromechanical phenomena.

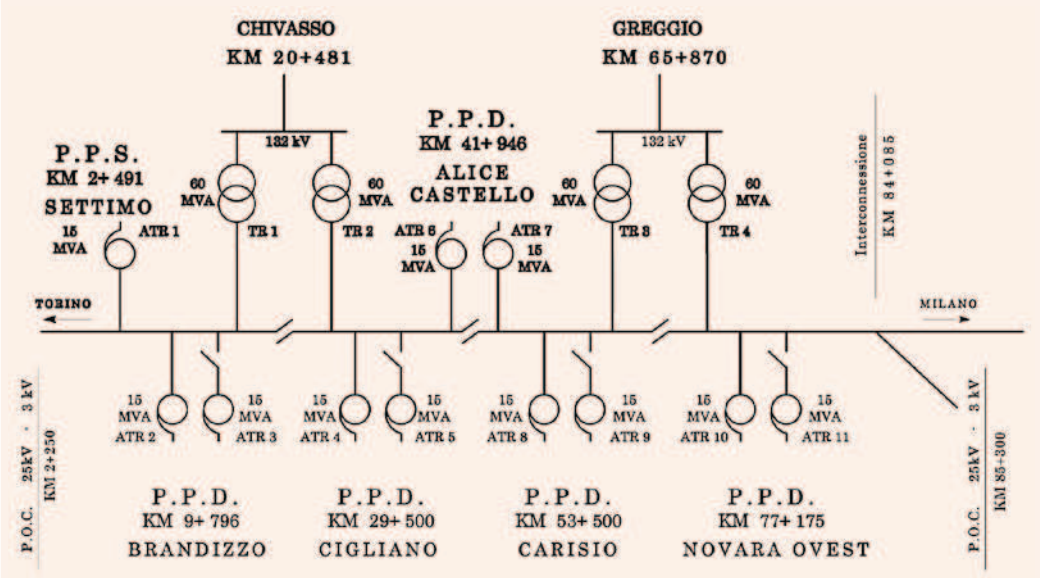

Fig. 21 - Traction supply single-line diagram – configuration with two transformers operating in each ESS

In cases 3 and 8 of Table 3, relevant to time-shifts of 0 and 2 minutes respectively, the two configurations yield the same results, as the train running the up-line (in braking phase) and the train running the down line (in traction phase) are located within the same line section (supplied by the transformer TR1 in the Chivasso ESS). When the time-shift is increased up to 4-8 minutes, the two trains falls within two different line sections, supplied by different transformers (namely TR1 and TR2 of Chivasso ESS), so that they cannot exchange any braking energy that is anyway fed back to the HV supply system through the ESS.

The absence of other loads (trains in traction phase) within the same line section makes the pantograph voltage of the braking train to exceed the standard limits thus imposing the rheostatic dissipation of part of the braking energy. This kind of analysis, also applicable to the Novara-side line sub-sections, explains the recovered energy reduction with respect to those case studies where the SSE neutral sections are operated in "closed" position (cases 13, 18 and 23 of Table 3).

Line operation with the ESS "neutral sections" in "open" position implies the subdivision of the line into electrically independent sections thus sharply reducing, being identical the traffic condition, the capability to transfer the braking train recoverable energy to the trains in traction phase.

Differences in the energetic parameters concerning the two traction supply system configurations become obviously appreciable only in high traffic density conditions (train headway not greater than 15 minutes); the traction supply system configuration with ESS "neutral sections" in "closed" position is anyway better suited to the application of regenerative braking in all possible traffic scenarios, because of the relevant increase in the train receptivity.

7. Conclusions

The integrated methodology presented in this paper allows an easy and systematic application of the powerful and reliable ATP-EMTP software to the simulation of 2x25 kV-50 Hz traction power supply systems. The ATP-EMTP, a universally accessible and internationally recognised tool, is suitable for the calculation of multiconductor, symmetrical or unsymmetrical, electric power systems, both in steady-state and in transient conditions.

This methodology was applied to the analysis of the Torino-Novara HS/HC line section, with a particular focus on the electric and energetic effects of train regenerative braking. The achieved results allowed to show the influence of some specific parameters on the recovered energy amount, such as train headway, time-shift between train departures at the two opposite ends of the line, ESS no-load voltages, maximum allowed pantograph voltage under braking conditions and the 25 kV traction power supply scheme

In particular, the parametric study showed the possibility to achieve a nearly global recovery of braking energy, with savings between 4% and 8% of overall energy demand. The not negligible

energetic implications of the regenerative braking phenomenon should suggest a deeper investigation about this system potentiality. The proposed procedure would allow a realistic evaluation, based on train paths, of the average recoverable energy in HS line sections, particularly in presence of mountain stretches or intermediate interconnections.

Acknowledgements

Authors thanks Eng. Claudio Sparvieri of RFI Technical Direction for his valuable collaboration in field data collection activity.

Prof. Ing. Alfonso Capasso
La Sapienza - University of Rome
Dipartment of Electrical Engineering

Dott. Ingg. Marco Ciucciarelli
La Sapienza - University of Rome
Dipartment of Electrical Engineering

Stefano Lauria
La Sapienza - University of Rome
Dipartment of Electrical Engineering

References

[1] G. Guidi Buffarini, E. Mingozzi, V. Morelli, "Criteri generali per l'alimentazione delle linee del sistema alta velocità italiano", AEI-Automazione Energia Informazione, vol. 8 n. 12, dicembre 1993, pp. 56-61.

[2] G. Guidi Buffarini, V. Morelli, "Criteri di progetto del sistema di trazione elettrica 25 kV, 50 Hz, per le nuove linee ferroviarie italiane ad alta velocità", Ingegneria Ferroviaria, novembre 1994.

[3] G. Guidi Buffarini, A. Colla, A. Fumi, "L'evoluzione degli impianti di trazione elettrica a 25 kV in Italia", Ingegneria Ferroviaria, gennaio 2009, pp. 9-32.

[4] A. Capasso, N. Ciaccio, R. Lamedica, A. Prudenzi, B. Perniceni, "Un modello semplificato per il calcolo elettrico dei sistemi di trazione ferroviaria 2×25 kV-50 Hz", Ingegneria Ferroviaria, luglio 1995, pp. 473-487.

[5] P. Firpo, S. Savio, G. Sciutto, "SIAV: un codice di calcolo automatico per l'analisi elettrica del sistema ad alta velocità 2×25 kV-50 Hz", Atti della Conferenza "Sviluppo e prospettive dei trasporti elettrificati: ricerca e innovazione", Genova, 25-27 novembre 1992, pp. 171-181.

[6] R.J. Hill, I.H. Cevik, "On-line simulation of voltage regulation in autotransformer-fed AC electric railroad traction networks", IEEE Trans. on Vehicular Technologies, vol. 42 n. 3, august 1993, pp. 365-372.

[7] A. Mariscotti, P. Pozzobon, M. Vanti, "Simplified modelling of 2×25 kV-50 Hz AT railway systems for the solution of low frequency and large-scale problems", IEEE Trans. on Power Delivery, vol. 22 n. 1, january 2007, pp. 296-301.

[8] G. Guidi Buffarini, "Impostazione generale del calcolo elettrico delle linee di contatto della trazione a corrente alternata", Ingegneria Ferroviaria, agosto 1983, pp. 505-514.

[9] G. Guidi Buffarini, "Il calcolo elettrico del sistema di trazione monofase 2×25 kV-50 Hz", Ingegneria Ferroviaria, novembre 1994, pp. 505-514.

[10] R. Benato, R. Caldon, A. Paolucci, "Algoritmo matriciale per l'analisi di una linea ferroviaria ad alta velocità e rispettiva rete di alimentazione", L'Energia Elettrica, vol. 75, n. 5, settembre-ottobre 1998, pp. 304-311.

[11] G. Cosulich, T. Ghiara, "Progettazione e verifica degli impianti per l'alimentazione dei sistemi di trasporto elettrificati", Ingegneria Ferroviaria, luglio 2005, pp. 505-519.

[12] G. Lucca, "Propagazione di tensione e corrente lungo un binario: due modelli di calcolo a confronto", Ingegneria Ferroviaria, febbraio 2005, pp. 133-143.

[13] A. Adinolfi, R. Lamedica, C. Modesto, A. Prudenzi, S. Vimercati, "Experimental assessment of energy saving due to trains regenerative braking in an electrified subway line", IEEE Trans. on Power Delivery, vol. 13 n. 4, october 1998, pp. 1536-1542.

[14] H-S. Wang, "Control strategy for optimal compromise between trip time and energy consumption in a high-speed railway", IEEE Trans. on Systems, Man and Cybernetics - Part A, vol. 28, n. 6, november 1998, pp. 791-802.

[15] Commissione Europea "Specifica tecnica di interoperabilità per il sottosistema «energia» del sistema ferroviario transeuropeo ad alta velocità", 2008/284/CE.